Journal of Sciences, Islamic Republic of Iran 19(3): 223-235 (2008) http://jsciences.ut.ac.ir
University of Tehran, ISSN 1016-1104

Post-Collisional Plio-Pleistocene Adakitic Volcanism in Centeral Iranian Volcanic Belt:Geochemical and Geodynamic Implications

G. Ghadami,[1,*] A.M. Shahre Babaki,[1] and M. Mortazavi[2]

[1]*Department of Geology, Faculty of Science, University of Shahid Bahonar, 76175-133 Kerman, Islamic Republic of Iran*
[2]*Department of Geology, Faculty of Science University of Hormozgan, 3995 Bandar Abass, Islamic Republic of Iran*

Abstract

In the Central IranianVolcanic Belt (CIVB), north-west of Shahre-Babak, in the area of Javazm, Dehaj and khabr, about 60 subvolcanic porphyritic dacitic to rhyodacitic domes (1-10 km^2) are intruded into a variety of rock sequences from Mesozoic to Early Miocene in age. These rocks are a part of Dehaj-Sardoieh belt. The CIVB contains intrusive and extrusive rocks of Cretaceous-Quaternary age. Geochemical data indicate that the subalkalic dacitic to rhyodacitic rocks have an adakitic composition with Na_2o/K_2o (1.8-3.16), high Sr (584-1750 ppm), Mg # = (0.18-0.57) and low Y (7-10 ppm), low Yb (0.65-1.29 ppm), and low HREE. Fractionated REE patterns, $(Ce/Yb)_N$ = 10-27, absence of negative Eu anomal, low content of Y, Nb, Ti, and high Sr/Y (74-265) and $(Ce/Yb)_N$ ratios suggest that the source was probably hydrous garnet-amphibolite or amphibole-eclogite, possibly generated during subduction of the Neo-Tethyan oceanic slab beneath the Central Iran microplate.The adakitic volcanism was followed by eruption of alkaline magmatism in this area. Slab melting occurred after cessation of subduction, possibility from the collision. Transtensional tectonics accompanied by a locally extensional stress regime account for magma genesis and ascent.

Keywords: Post-collision; Dacite; Adakite; Neo-Tethys; Iran

Introduction

The Tethyan orogenic collage formed from collision of dispersed fragments of Gondwana with Eurasia [8-33-44-53-62]. Within this context, three major tectonic elements with NW-SE trends are recognized in Iran due to collision of Afro-Arabian continent and Iranian microcontinent. They include the Central Iranian Volcanic Belt (CIVB), Sanandaj-Sirjan metamorphic zone and Zagros-folded-thrust belt (Fig. 1) [2-44-65]. The CIVB contains intrusive and extrusive rocks of Cretaceous -Quternary age that forms a belt with 50 Km wide and 4 Km thick [6] that extends from NW to SE in Iran. However, peak of magmatic activity is thought to

* Corresponding author, Tel.: 09368845513, Fax: +98(341)3222035, E-mail: ghadamigholamreza@yahoo.com

be Eocene age [3-23-67]. Geochemical studies indicate that the CIVB is generally composed of subduction-relate calc-alkaline rocks [8-24-34]. Alkaline rocks also are reported locally by [4], [29] and [45]. [4], proposed a rift model to interpret the genesis of Eocene magmatic rocks in the CIVB. [6] argued that the onset of alkaline volcanism, which followed the calc-alkaline volcanism (6-5 Ma) in CIVB was due to sinking of the final broken pieces of oceanic slab to a depth where alkaline melts were generated. [25] suggested that post-suturing magmatic activity along the Sanandaj-Sirjan zone and CIVB can be attributed to slab break-off.

In CIVB, area of Javazm, Dehaj and Khabr a geologic complexity and magmatic activity from calc-alkaline to alkaline presented. The diversity of magmatic types from calk-alkaline to alkaline indicate region of Javazm, Dehaj and Khabr to represent classical areas of young volcanism. The most intense eruptions were during the post collisional stage, which led to the formation of great volcanoes like Mosahim, Madvar, Aj Bala, Aj Pain and other volcanoes in this region.

The great diversity of Neogene to Quaternary magmatic rocks, from andesitic, dacitic to rhyodacitic subvolcanic domes and extending for more than 150 km, are of interested due to their specific conditions of formation and spatial and temporal relation with other magmatic rocks. The dacitic volcanism of late Pliocene and Pleistocene in this area was followed by alkaline volcanism in Plio-Quaterner [33]. A conspicuous characteristic of this phase is the contemporaneous eruptions of mafic alkaline melts including melafoidites and alkali basalts [7-29]. The temporal and spatial relationship of dacitic calc-alkaline magmatism with alkaline volcanism is also reported from different areas of Gondwana fragments and Eurasia plate collision zone [12-48-58].

The aims of this paper are (1) to present chemical characteristics of the dacitic to rhyodacitic magmatism in central Iran, (2) to suggest the conditions of their genesis, and (3) to discuss geodynamic environment in which they could have formed.

Material and Methods

2.1. Regional Setting

The investigated areas are situated at the Central Iranian Volcanic Belt (CIVB), north west of Shahre-Babak City (Fig. 1-3). These regions are situated between Rafsanjan fault and Nain-Baft fault (Shahre-Babak fault) (Fig. 2). In this area, numerous (n~50) subvolcanic domes are intruded in to the volcanic Eocene, Oligocen and volcano-sedimentary rocks of CIVB, (Fig. 3). In the south-west of the Khabr subvolcanic domes intruded in to the ophiolitic rocks. The ophiolitic rocks belong to Nain-Baft ophiolite. The field study and the comparison of Figures 2 and 3, indicate that these andesitic and dacitic rocks were emplaced along faults and fractures. It is believe that the ascent of acidic magma may be relate to the fault activity in this area (Fig. 3).

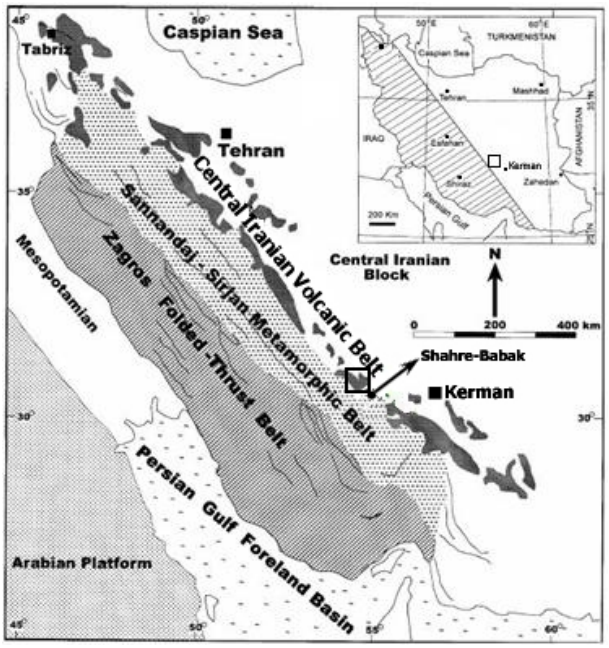

Figure 1. Three main tectonic units of the Zagros orogenic belt [2-44]; ☐ Studied area.

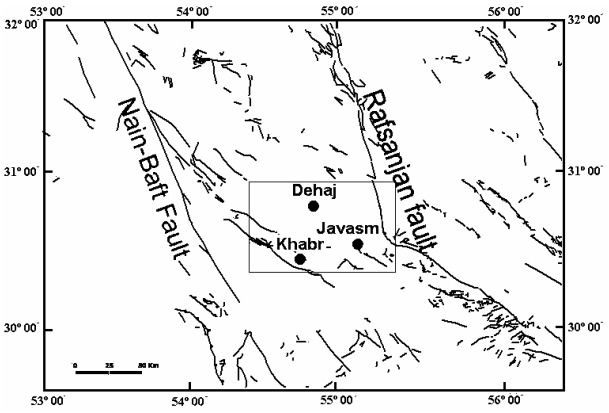

Figure 2. Tectonic map of the studied area that show by a square, studied area bounded by two main faults and fractures [19,20].

The Eocene volcanic and volcaniclastic rocks consist of basalt, andesitic-basalt, brecciated volcaniclastic rocks and green tuffs. The oligocen dioritic plutons consist of porphyritic diorite, granodiorite and quartes-diorite rocks.The ophiolite rocks situated are east of the Khabr and consist of basalt,gabbro,serpantine and pelagic sediment, and age of this rocks are Cretaceous and was emplaced before the Paleocene [19]. The age of emplacement of subvolcanic domes are Plio-Pleistocene [19-20], but has been determined by [45], which yield ages 7-17 Ma based on Amphiobol and Biotite on K/Ar dating methods. Field studies indicate that these domes were emplaced along faults and fractures that developed in shear zone with the Nain-Baf (Share Babak) fault in south and Rasanjan fault in north of region (Fig. 2). Strike-slip tectonics accompanied by a transtensional regime may also account for generation of adakitic and alkaline magmatisme in this area. Alkaline magmatisme related to Plio-Quaterner [7-29].

2.2. Petrographic Features

The porphyritic volcanic rocks consist of intermediate to felsic suites whose composition varies from hornblende-andesite, dacite and rhyodacite. Dacitic and rhyodacite rocks are dominant and show porphyritic texture with phenocrysts of plagioclase, hornblende and biotite. Plagioclase is ubiquitous phenocryst (25-50 vol %) and contains inclusions of magnetite, amphibole and opaque. Andesites and dacites contain large plagioclase crystals (3-5 mm) that usually exhibit sieve textures and well defined zoning marked by concentric zones rich in/or devoid of glass and opaque inclusion. In some samples, plagioclase phenocrysts are mantled by a rim devoid of inclusions, whereas the core is rich in inclusions.

Hornblende occurs as the main ferromagnesian phenocryst (up to 2 mm) in andesite and dacite and varies from green to brown in color. Hornblend often opassitezed and change to opaque and iron oxide. In some samples, accumulation of hornblende led to formation of glomeroporphyric texture. The groundmass is composed of plagioclase and hornblend as the main minerals, with apatite, biotite, quartz and iron oxides as accessory minerals.

2.3. Geochemical Characteristics

2.3.1. Analytical Methods

About 200 samples of the dacitic rocks were collected from different domes. In order to correctly characterize their chemical composition, 29 samples were chosen for major, trace and rare-earth elements (REE) analysis. Samples for whole rock analysis were crushed and powdered in agate ball-mills. Major elements were determined by ME-ICP method. Inductively Coupled Plasma-Mass Spectorometry (ICP-MS) was employed for REE and trace element analysis for all of the samples. All of the analysis were determined at Actlabs laboratories (Canada). Represen-tative chemical analysis for major, trace and rare earth elements are presented in Tables 1, 2 and 3.

2.3.2. Analytical Results

The SiO_2 of samples vary from 59 to 67.5 wt %. Using SiO_2 vs. Zr/TiO_2 diagram of [71] for classification of volcanic rocks, the studied samples plot in the fields of andesite and dacite-rhyodacite (Fig. 4). Also these rocks are metaluminous with $Al_2O_3/(CaO+Na_2O+K_2O)$ ratios of 1.5-2.0.

Using SiO_2 as a fractionation index, the samples display chemical variation and clear trends on Harker diagrams (Fig. 5). On variation diagram FeOt, MgO, TiO_2, CaO, MnO and P_2O_5 display negative correlations, suggesting that these volcanic rocks experienced fractionation of apatite, hornblende and plagioclase. The scattered of the samples belong to present of phenocryst (fractional crystallization) or assimilation of continental crust. The other oxides and elements (e.g. K_2O, Na_2O, Zr, Ba and etc.) display scatter trends.

The K_2O/Na_2O ratios vary from 0.32 to 0.63 and samples are plot in the medium-potassium field and

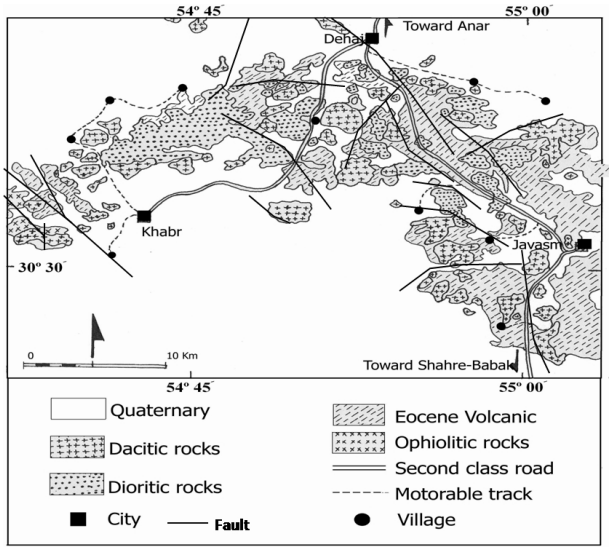

Figure 3. Geological map of area (Simplified from the geological map of 1: 250000 Anar), [19].

high potassium field (Fig. 6). In the AFM diagram of [32], (Fig. 7).In diagram Na2O+K2O vs. SiO2 [32], all of the samples plot in subalkaline field (Fig. 8). In Y vs. Zr diagram [37] the sample plote in the calc-alkaline field (Fig. 12). The Mg # [MgO/(MgO+FeO)] of the samples ranges from 0.18 to 0.57 and contain high concentration of Sr (584 to 1750 ppm) and low contents of Y and Rb. The high contents of Sr, high ratios of K_2O/Na_2O, Mg # (mean 0.42) and concentrations of Rb and Y indicate geochemical characteristics different from typical volcanic rocks.

In the Y vs. Sr/Y diagram, all of the samples plot in the field of adakite relative to typical arc-related calc-alkaline rocks defined by [15], (Fig. 9). In the $(La/Yb)_N$ vs. Yb_N diagram all of the samples plot in the field of adakite relative to classical island arc rocks defined by [40], (Fig. 10). Figure 13 shows a spider diagram plot for representative samples from different domes normalized to primitive mantle composition [68]. All of the samples exhibit typical subduction-related signatures: they are enriched in large ion lithophile elements such as K, Rb and Ba and light REE relative to HFSE and HREE and negative Nb anomalies. They show significant positive anomalies for Sr, indicative of either the absence of plagioclase fractionation or retention of plagioclase in the residue. The adakites exhibit Sr enrichment, in contrast to non-adakitic dacities and rhyodacites which show negative anomalies inspider diagrams.

Figure 14 displays the incompatible element patterns of representative samples normalized to average N-MORB of [68]. LILE and LREE enrichment can result from low degree partial melting of a MORB source. Decoupling of Zr and Ti with similar bulk Kd's and greater depletion of Ti has been interprete to reflect a

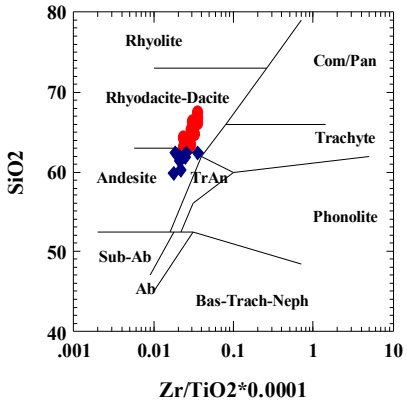

Figure 4. Classification of volcanic rocks by Zr/TiO_2 vs. SiO_2 [71]. Studied samples compositions range from Andesite, to dacite-rhyodacitic.

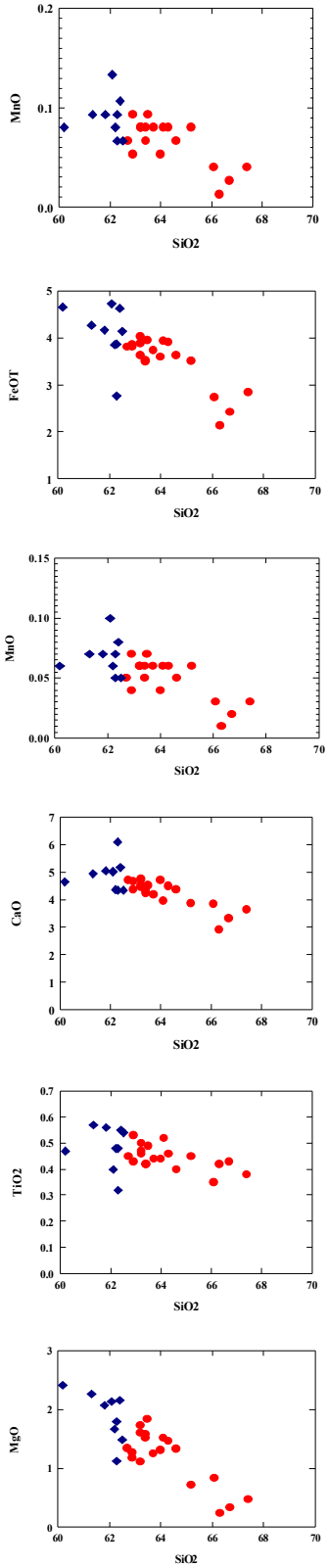

Figure 5. Variation diagrams for major and trace elements of samples ♦ Andesite, ● Dacite.

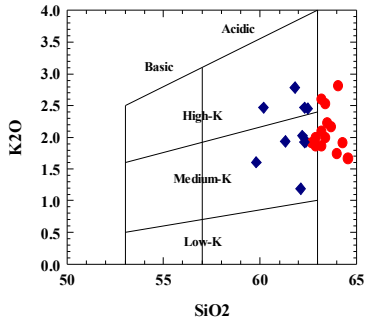

Figure 6. K_2O vs. SiO_2 for dacitic rocks of Central Volcanic Belt of Iran. Most of the samples plat in medium-k field and high-K[26], ♦ Andesite, ● Dacite.

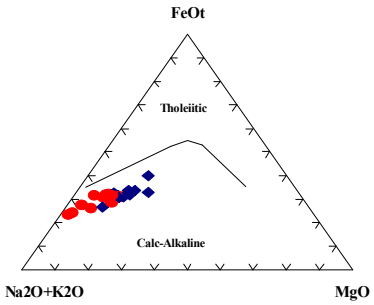

Figure 7. AFM diagram of [32]. All of the samples plot in Calc-Alkaline field, ♦ Andesite, ● Dacite.

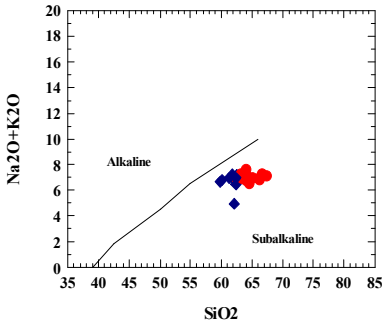

Figure 8. Na_2O + K_2O vs. SiO_2 diagram [32], all of the samples plot in subalkaline field, ♦ Andesite, ● Dacite.

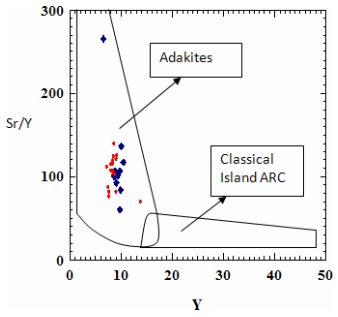

Figure 9. Sr/Y vs. Y diagram [15] discriminating between adakitic and classical arc calc-alkaline compositions, ♦ Andesite, ● Dacite.

residual phase in the source that fractionated Ti [47] or Ti-bearing phases [52]. The strong depletion of Y and Yb corresponds to presence of restite garnet in the eclogitic source. The REE concentrations for samples of adakitic rocks from study area are plotted relative to chondrite in Figure 15. The ∑REE ranges from 61 to 173 ppm. The REE patterns for adakitic rocks from the study area are similar, although the abundances are variable. All the samples are enriched in LREE and strongly fractionated in LREE and have a flat MREE to HREE pattern (La_N/Yb_N values of 11 to 38). The REE patterns for the rocks from the study area are linear with a small positive Eu anomaly, implying their cogenetic nature and derived from source regions that had similar relative concentrations of REE and similar mineralogy. Also the parallel nature of the REE patterns established that the residues had a big partition coefficient for these elements, and consequently that they were grant. Low abundances of HREE in adakitic magma reflect retention of these elements in residual garnet in the partially melted subducted slab amphibol-eclogite. There are no cross-cutting REE patterns, suggesting that the studied magmatic suites are possibly related to and most likely derived from the same initial melt.

Results and Discussion

3.1. Discussion

The degree to which anatexis of subducted oceanic crust has contributed to magmatism in convergent plate margins has been a point of controversy for decades [18]. As discussed by [26], arc magmas of basaltic composition are regarded as products of mantle, not slab anatexis, although some later workers continued to press for slab anatexis in the production of arc basalts, particulary those with high Al-contents [41]. Hydrated mantle peridotite as the principal source for arc basalts is now firmly established [69], but genesis of intermediate and felsic are magmas remains controversial.

The issue of slab anatexis as a globally important process was emphasized by [15] and [21] who demonstrated a connection between subduction of young oceanic crust and production of intermediate to felsic igneous rocks which bear the signature of a garnetiferous residuum. Such magmatic rocks are compositionally similar to Tertiary lavas on Adak Island in the Aleutian arc which were identified as products of slab melting by [35]. This petrologic family, termed "*adakites*", was described by [15] as high-alumina, intermediate to felsic volcanic rocks typically hosting phenocrysts of plagioclase, amphibole, mica and

Table 1. Major and trace element contents of representative adakitic samples of CIVB

Sample	1-1	2-1	9-1	11-5	13-1	18-5	19-6	20-1	21-2	24-2	24-10	28-2	30-1	31-4	33-3
Rock type	An	An	Da	Da	Da	An	Da	Da	Da	Da	Da	Da	Da	An	Da
SiO_2	62.1	62.2	64	62.9	63.4	62.4	63.2	66.7	62.9	62.7	64.3	67.4	66.1	61.3	65.2
Al_2O_3	16.15	16.2	16.4	16.7	16.45	17.5	16.65	16.15	16.6	16.2	16.9	15.95	15.55	16.4	16.8
Fe_2O_3*	4.27	3.86	3.6	3.81	3.52	4.62	3.63	2.42	3.86	3.81	3.91	2.84	2.74	4.27	3.51
CaO	5.03	4.37	4.71	4.66	4.35	5.16	4.64	3.32	4.36	4.72	4.5	3.63	3.83	4.94	3.87
MgO	2.14	1.67	1.31	1.18	1.52	2.16	1.12	0.33	1.27	1.34	1.46	0.48	0.84	2.27	0.72
Na_2O	3.76	4.76	5.03	5.22	5.1	5.08	5.17	4.73	4.96	4.91	5.15	4.6	4.54	5.03	4.63
K_2O	1.19	2.02	1.73	1.86	2	1.93	1.86	2.5	1.99	1.91	1.91	2.49	2.38	1.93	2.36
Cr_2O_3	0.03	0.03	0.02	0.02	0.03	0.02	0.02	0.04	0.02	0.04	0.04	0.02	0.02	0.02	0.03
TiO_2	0.4	0.48	0.44	0.43	0.42	0.55	0.46	0.43	0.53	0.45	0.46	0.38	0.35	0.57	0.45
MnO	0.1	0.06	0.04	0.07	0.06	0.08	0.06	0.02	0.04	0.05	0.06	0.03	0.03	0.07	0.06
P_2O_5	0.13	0.22	0.19	0.15	0.2	0.2	0.22	0.19	0.31	0.19	0.19	0.17	0.16	0.29	0.2
lOI	3.18	2.17	1.86	2.54	2.97	0.69	0.93	1.22	1.17	1.54	0.98	1.73	1.33	1.34	2.03
Total	99	98.2	99.5	99.8	100	100	98.1	98.2	98.2	98	100	99.9	98	98.7	100
Na_2O/K_2O	3.16	2.36	2.91	2.81	2.55	2.63	2.78	1.89	2.49	2.57	2.7	1.58	1.91	2.61	1.96
Mg#	0.47	0.46	0.42	0.38	0.46	0.48	0.46	0.21	0.39	0.41	0.42	0.25	0.38	0.51	0.29
Ba	395	596	561	687	676	640	647	657	700	632	627	635	629	713	642
Cr	210	240	140	90	190	150	160	330	130	280	310	130	130	130	180
Cs	1.33	0.93	0.71	0.67	0.85	1.44	1.09	2.27	0.82	1.8	1.36	2.13	1.96	1.19	2.88
Cu	21	38	40	23	42	54	25	44	35	49	43	45	40	43	43
Ga	19	20.6	20.5	20.5	21.3	21.6	21.1	21.9	20.8	21.3	21.1	20.7	20.3	20.6	20.6
Hf	2.4	3.1	3.1	3.2	3.1	3.1	3.2	4	3.4	3.1	3.2	3.6	3.6	3.4	3.8
Mo	6	5	4	2	3	3	4	10	3	5	9	3	3	3	3
Nb	2.5	4.7	4.5	5.8	5.3	5.6	5	6.3	7.2	5	5	5.4	5.3	9.5	6.2
Ni	17	26	16	14	23	42	17	23	29	25	23	14	12	30	16
Pb	8	14	12	12	15	13	12	16	15	13	14	16	19	13	17
Sr	584	950	913	1175	979	1040	1005	662	1225	942	945	633	585	1230	745
Rb	26.3	32.5	33.4	29.4	39.4	39.8	37.1	65.3	38	42.7	41.4	63.2	62.4	35.5	60.4
Ta	0.4	0.4	0.5	0.5	0.5	0.5	0.5	0.6	0.6	0.5	0.5	0.6	0.6	0.7	0.7

*Fe_2O_3 as total Fe_2O_3. Majer elements Wt %, trace elements and REE in ppm. An: Andesite, Da: Dacite-Rhyodacite.

(rarely) orthopyroxene, and lacking phenocrysts of clinopyroxene. Accessory grains of titanomagnetite, apatite, zircon and titanite were identified as common but not ubiquitous.

A complementary and broadly accepted chemical definition of adakites was sub-sequently provided by [16]: adakites are high-silica (SiO_2>56%), high-alumina (Al_2O_3>15%), plagioclase and amphibole-bearing lavas with Na_2O>3.5%, high Sr (>400ppm), low Y (<18ppm), high Sr/Y (>40), low Yb (<1.9), and high La/Yb>20.

Geochemically, it appears that subduction related components played a controlling role in the genesis of the dacitic magmas in Central Volcanic Belt of Iran (CIVB). Enrichment of LILE and depletion of HFSE (Nb and Ti) and HREE are characteristic of subduction zone magmatism [15-16-39-40-70]. on the other hand the high ratios of Na_2O/K_2O, high Sr, Mg #, Sr/Y and $(Ce/Yb)_N$ suggest an adakitic character for subduction-related magmatism [15-16-69-40].

The origin of adakites has been attributed to partial melting of either subducted oceanic crust converted to eclogite and garnet amphibolite [15-21-35-38-39], or underplating of basaltic magmas under thick continental crust [5].

The strongly fractionated REE pattern and depletions HREE and Y in adakites are possibly due to the

Table 1. Continued

Sample	1-1	2-1	9-1	11-5	13-1	18-5	19-6	20-1	21-2	24-2	24-1	28-2	30-1	31-4	33-3
Rock type	An	An	Da	Da	Da	An	Da	Da	Da	Da	Da	Da	Da	An	Da
Th	2.5	4.86	3.96	5.66	4.87	4.2	4.16	6.94	11.35	4.18	4.16	6.63	6.63	7.16	7.15
U	1.13	1.46	1.33	1.67	1.67	1.42	1.42	2.67	2.91	1.47	1.47	2.65	2.33	2.09	2.71
V	106	93	80	62	74	101	86	74	99	84	90	60	56	97	67
W	4	12	5	6	11	3	4	9	3	15	8	6	5	6	13
Y	9.7	9.4	9	9.5	8.6	9.8	8.6	7.8	8.9	8.8	8.4	7.9	7.9	10.5	9.3
Zr	81	114	110	115	115	104	120	153	125	111	109	135	124	120	135
Ti	2400	2880	2640	2580	2520	3300	2760	2580	3180	2700	2760	2280	2100	3420	2700
P	567	960	829	654	873	873	960	829	1353	829	829	742	698	1266	873
Rb/Sr	0.05	0.03	0.04	0.03	0.04	0.04	0.04	0.1	0.03	0.05	0.04	0.1	0.11	0.03	0.08
Sr/Y	60.21	101	101	123.7	113.9	106.1	116.9	84.5	137.7	107	112	80.2	74	117	80
La	12	24.5	20.7	28.6	24.5	23.3	22	26.1	42.3	20.5	20.1	23.3	21.9	36	24.4
Ce	24.7	46.7	40.3	55.2	45.2	44.3	43.3	49.6	78.7	40.5	40	43.3	40.8	69.2	44.3
Pr	2.8	5.04	4.42	5.8	4.82	4.95	4.76	5.25	8.2	4.49	4.38	4.56	4.22	7.3	4.7
Nd	11.4	19.3	16.9	21.4	18.2	19.2	18.4	19	29.8	17.2	16.6	16.4	15.7	27	17.5
Sm	2.29	3.57	3.14	3.79	3.33	3.5	3.38	3.38	4.64	3.41	3.1	2.95	3	4.62	3.49
Eu	0.83	1.04	1	1.08	0.98	1.08	0.98	0.96	1.38	0.92	0.96	0.89	0.83	1.32	1.06
Gd	2.23	2.96	2.79	3.36	2.75	3.22	3	2.66	3.91	2.92	2.73	2.58	2.71	4.11	3.15
Tb	0.33	0.39	0.37	0.42	0.35	0.41	0.37	0.33	0.48	0.35	0.37	0.35	0.34	0.5	0.42
Dy	1.84	1.85	1.85	1.98	1.69	2.05	1.17	1.6	1.99	1.76	1.81	1.57	1.83	2.32	2.01
Ho	0.34	0.34	0.35	0.35	0.28	0.36	0.33	0.27	0.33	0.32	0.33	0.28	0.32	0.4	0.38
Er	0.98	0.97	0.97	1.08	0.93	1.02	0.87	0.8	0.95	0.94	0.98	0.84	0.88	1.17	1.08
Tm	0.12	0.12	0.13	0.13	0.1	0.13	0.11	0.09	0.1	0.12	0.12	0.11	0.12	0.14	0.14
Yb	1.01	0.84	0.89	0.88	0.73	0.8	0.76	0.65	0.75	0.84	0.81	0.8	0.81	0.91	0.99
Lu	0.14	0.12	0.12	0.13	0.1	0.12	0.1	0.1	0.09	0.09	0.11	0.1	0.12	0.15	0.15
$(La/Yb)_N$	15.65	19.62	15.67	22.26	23	19.84	19.97	27.35	38.4	16.41	17.09	19.81	18.36	27.25	16.63
$(Ce/Yb)_N$	6.45	14.35	11.69	16.49	16.28	14.5	15	19.9	27.4	14.44	13	14.1	13.31	20	11.6
∑ REE	61	107.7	93.93	124.2	103.5	104.5	100.1	110	173	94.4	92.4	98	93.5	155	103.7

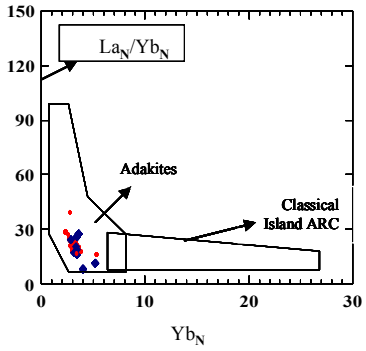

Figure 10. $(La/Yb)_N$ vs. Yb_N diagram [39] discriminating between adakitic and classical arc calc- alkaline compositions, ♦ Andesite, ● Dacite.

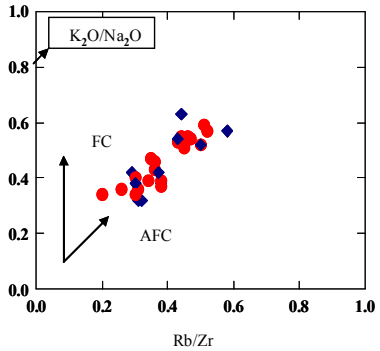

Figure 11. Diagram of K_2O/Na_2O vs. Rb/Zr shows fractional crystallization (FC) and assimilation fractional crystallization (AFC) trends [22], ♦ Andesite, ● Dacite.

Table 2. Major and trace element contents of representative adakitic samples of CIVB

Sample	35-d	38-1	46-4	48-4	50-2	52-3	54-3	55-2	58-1	60-2	63-4	64-1	65-2	68-1a
Rock type	Da	Da	An	An	Da	Da	An	An	Da	Da	Da	An	An	Da
SiO_2	63.7	63.2	65.3	59.8	66.3	63.5	62.5	61.8	64.1	63.4	63.2	62.3	60.2	64
Al_2O_3	16.8	16.55	14.95	16.2	17.65	16.4	17.2	16.05	16.4	16.2	16.4	16.05	16.35	15.8
Fe_2O_3*	3.74	3.88	2.77	4.79	2.14	3.95	4.14	4.17	3.94	3.49	4.03	3.87	3.66	3.36
CaO	4.2	4.51	6.1	6.1	2.92	4.52	4.34	5.04	3.97	4.24	4.74	4.33	4.64	4.36
MgO	1.26	1.6	1.13	3.22	0.24	1.84	1.48	2.07	1.52	1.58	1.73	1.8	2.42	1.33
Na_2O	4.76	4.92	4.52	5.05	4.35	4.7	4.69	4.44	4.76	4.58	4.68	4.53	4.35	4.9
K_2O	2.17	2.1	1.92	1.61	2.47	2.22	2.45	2.78	2.81	2.53	2.59	2.46	2.47	1.66
Cr_2O_3	0.02	0.03	0.02	0.03	0.02	0.04	0.02	0.02	0.01	0.02	0.03	0.02	0.02	0.02
TiO_2	0.44	0.47	0.32	0.61	0.42	0.49	0.54	0.56	0.52	0.42	0.5	0.48	0.06	0.05
MnO	0.06	0.06	0.05	0.08	0.01	0.07	0.05	0.07	0.06	0.05	0.06	0.07	0.06	0.05
P_2O_5	0.23	0.24	0.15	0.27	0.15	0.24	0.26	0.26	0.23	0.2	0.22	0.19	0.2	0.17
lOI	2.4	2.44	5.48	2.16	3.15	1.74	2.13	2.6	1.22	2.3	1.72	1.93	2.17	1.29
Total	100	100	100	100	100	99.9	100	100	99.8	99.2	100	98.2	98.2	98.1
Na_2O/K_2O	2.19	2.34	2.35	3.14	1.76	2.12	1.91	1.6	1.69	1.81	1.81	1.84	1.76	2.95
Mg#	0.4	0.45	0.44	0.57	0.18	0.48	0.41	0.49	0.43	0.47	0.46	0.48	0.5	0.4
Ba	781	713	653	659	1025	695	764	645	654	605	615	585	826	493
Cr	120	240	150	180	120	250	120	180	130	190	250	160	180	170
Cs	1.9	1.72	1.72	1.13	4.99	2	1.68	1.34	2	1.48	1.47	1.28	2.48	0.64
Cu	29	39	39	48	20	36	44	38	17	23	40	46	59	53
Ga	20.3	20.7	19.1	20.5	20.3	20.4	21.4	19.4	19.7	19	20.1	20.5	19.5	21.2
Hf	3.3	3.8	3.5	3.5	3.8	3.6	3.4	3.6	3.7	3.4	3.4	3.3	2.8	3.6
Mo	4	5	4	3	3	4	3	2	2	5	4	4	2	5
Nb	5.8	6.3	4.4	6.7	7.8	7.6	6.9	11.1	10.3	8.2	8	7.6	4.9	4
Ni	17	30	16	59	15	26	11	33	20	19	29	26	36	15
Pb	13	13	12	11	17	15	17	14	14	13	11	15	12	11
Sr	1125	1080	1750	1385	955	873	975	827	862	886	905	873	832	820
Rb	39.9	40.6	41.8	33.6	66.2	43.8	62	60.4	66.8	56.5	54.7	52.9	58.7	26.5
Ta	0.5	0.6	0.6	0.7	0.7	0.7	0.6	0.8	0.7	0.6	0.6	0.6	0.4	0.3

*Fe_2O_3 as total Fe_2O_3. Majer elements Wt %, trace elements and REE in ppm. An: Andesite, Da: Dacite-Rhyodacite.

presence of garnet +/− amphibole in melt residue. Their high Sr and low Nb, Ta, and Ti contents are thought to be due to absence of plagioclase and presence of Fe-Ti oxides in the residue [39]. While geochemical data for igneous rocks compiled by [15] indicate a relationship between subducted oceanic crust and adakite genesis, adakite occurrences in different tectonic environment lad [42] to propose that slab melting even of old oceanic crust is also possible during: 1- The initiation of subduction [55-56]. 2- Fast and oblique subduction [35-46]. 3- Termination of subduction [49-57].

The high Mg and Cr content of most adakites are not consistent with the low concentration of these elements in experimentally produced melts of amphibolite or eclogite[50- 61]. [60]and [73] attributed this enrichment to the interaction of adakitic magma with the mantle during ascent. Experimental work by [51] show that small amounts of adakitic melt are entirely consumed in reaction with mantle peridotite to from metasomatised zones as has been proposed by [59] and [61].

On the other hand, when the ratio of melt/peridotite reaches 2:1, a portion of melt not consumed in the reaction becomes Mg-enriched and preserves its trace-element geochemical characteristics such as high Sr/Y and $(Ce/Yb)_N$ ratios.

The highly enriched N-MORB normalized

Table 2. Continued

Sample	35-d	38-1	46-4	48-4	50-2	52-3	54-3	55-2	58-1	60-2	63-4	64-1	65-2	68-1a
Rock type	Da	Da	An	An	Da	Da	An	An	Da	Da	Da	An	An	Da
Th	5.24	5.44	6.94	4.66	3.85	7.71	4.77	7.14	7.56	7.11	6.58	6.45	8.15	4.1
U	1.86	1.76	2.15	1.45	3.96	2.03	1.73	2.31	2.41	2.23	2.08	1.96	2.97	1.22
V	78	78	55	109	67	79	85	89	100	76	84	86	110	62
W	4	11	9	6	7	13	8	7	7	7	11	4	9	5
Y	9.4	8.8	6.6	10.1	14.1	9.1	9.3	9.9	8.6	8.4	8.7	8.7	9	7.4
Zr	111	114	113	109	127	125	125	138	132	122	123	122	102	133
Ti	2640	2820	1920	3660	2520	2940	3240	3360	3120	2520	3000	2880	2820	2400
P	1004	742	654	1178	654	1047	1135	1135	1004	873	960	829	873	742
Rb/Sr	0.04	0.04	0.02	0.02	0.07	0.05	0.06	0.07	0.08	0.06	0.06	0.06	0.07	0.03
Sr/Y	119	122	165	137	67.7	95.9	105	83.6	100	105	104	100	92.5	109
La	26.3	27.4	20.1	25.2	30.2	27.2	24.7	32.6	26.4	25.3	25	25.2	23.4	25.2
Ce	49.6	49.9	35.7	50.5	57.7	49	46.2	51.8	48	46.5	48.2	47.6	42.6	43.3
Pr	5.37	5.38	3.77	5.58	6.17	5.2	5.17	5.85	5.36	5.14	5.5	5.44	4.82	5.06
Nd	19.9	20.1	13.8	21.5	24.3	19.3	19.1	22.1	20	19.6	20.4	20.6	18.2	19.3
Sm	3.51	3.48	2.67	4.2	4.86	3.44	3.36	3.73	3.37	3.24	3.45	3.46	3.2	0.93
Eu	1.08	1.17	0.88	1.4	1.47	1.07	1.12	0.95	0.92	0.91	0.94	0.99	0.96	0.93
Gd	3.32	3.26	2.69	3.93	4.56	3.03	3.3	3.14	2.87	2.8	2.95	2.92	2.84	2.84
Tb	0.42	0.44	0.31	0.5	0.62	0.41	0.39	0.41	0.36	0.33	0.34	0.37	0.35	0.33
Dy	1.97	2.09	1.63	2.43	2.96	1.89	2.16	1.89	1.72	1.67	1.74	1.81	1.88	1.51
Ho	0.37	0.35	0.28	0.44	0.56	0.33	0.36	0.34	0.29	0.27	0.31	0.3	0.32	0.27
Er	1.08	1.03	0.83	1.37	1.54	1.06	0.99	1.02	0.91	0.85	0.92	0.87	0.97	0.7
Tm	0.15	0.14	0.13	0.2	0.21	0.14	0.13	0.14	0.11	0.12	0.11	0.12	0.12	0.09
Yb	0.95	0.93	0.81	1.29	1.37	0.85	0.82	0.85	0.71	0.73	0.75	0.71	0.84	0.63
Lu	0.15	0.13	0.14	0.22	0.21	0.15	0.11	0.13	0.12	0.09	0.1	0.11	0.12	0.07
$(La/Yb)_N$	18.84	20.16	17.09	11.27	14.95	21.79	20.39	26.12	25.68	23.76	3.48	24.5	18.74	27.44
$(Ce/Yb)_N$	13.63	14	11.66	10.15	10.96	15.26	16.64	15.91	17.89	16.76	17.31	17.75	13.09	18.08
∑ REE	114.2	115.8	83.74	118.7	136.7	113.7	107.9	124.9	111.1	107.5	110.7	110.5	100.3	103.6

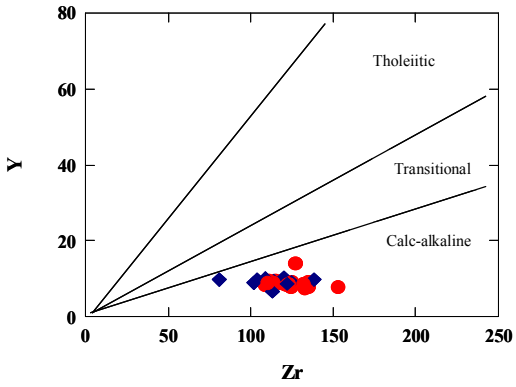

Figure 12. Diagram of Zr vs.Y after [36] all samples plot in the calc-alkaline field, ♦ Andesite, ● Dacite.

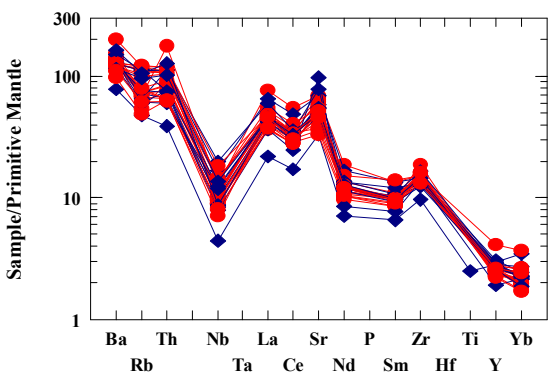

Figure 13. Primitive mantle-normalized incompatible trace element diagram for all samples [68] ♦ Andesite, ● Dacite.

abundance patterns of trace elements and REE pattern for adakitic dacitic and rhyodacites of CIVB (area of Javazm, Khabr and Dehaj) suggest the existence of garnet as a residue in the source. The enrichment of Sr and the absence of negative Eu anomalies indicate that the residual source was pelagioclase free. The Nb and Ti are strongly depleted in the studied samples, which suggest that the source also has residual rutile and amphibole and thus was most probably hydrous garnet-amphibolite or amphibole-eclogite. This garnet-bearing source implies that there are at least two possibilities for generation of adakitic rocks in Central Iran:

1. Partial melting of thickened lower crust and
2. or melting of subducted oceanic slab of Neo-tethys.

It is expected that crustal thickening caused by Arabian-Asian continental collision would result in transformation of basaltic lower crust in to garnet-amphibolite or amphibole-eclogite. However, such deeper crustal materials have not been observed nor reported as xenoliths from the studied area. Moreover, according to the Moho depth map of [14] the crustal thickness of the area ranges from 48 to 50 Km. A seismic refraction profile through Sar Cheshmeh [27], however, gave crustal thicknesses of only 30 to 40 Km for the CIVB in Kerman province, which is not an adequate depth for conversion of basaltic lower crust in to garnet- amphibolite or amphibole-eclogite.

The other candidate hydrous amphibole-eclogite or garnet-amphibolite, which could melt to generate adakitic magmas in central Iran, is subducted Neo-Tethyan oceanic slab. The andesitic, dacitic and rhyodacitic of study area show high Na_2O/K_2O, high Sr, low Y, strongly high REE depletion and high LREE. [46-60-61] believe that such compositional behavior of this rocks is consistent with their generation by melting of subducting oceanic lithosphere. The values of radiogenic Sr (0.704273 to 0.705668) and $\acute{\varepsilon}_{Nd}$ (+ 1.3 to +4.1) for this rocks from [45] respectively indicate that pelagic sediment could not have been involved in the genesis of the andesitic and dacitic rocks. Partial melting of an amphibole-eclogite sourse would generate melts that have high Sr/Y, high LREE, but low Y and low HREE [15-16-39-40].

Controversy exists in the literature about the timing of the closure of Neo-Tethyan along the Zagros suture. Some authors infer a late cretaceous age for continental collision [2-7]. A late Cretaceous age for continent-continent collision comes from the timing of the ophiolite emplacement, i.e. age of the youngest pelagic fossils involved in the Zagros ophiolites. However, this age has been shown to merely reflect the timing of ophiolite abduction due to collision of passive margin of Zagros-Oman an offshore intra-oceanic are [9], while a vast area of oceanic lithosphere still existed to the north of Zagros [17] yet to be subducted underneath central Iran during the Tertiary.An alternative idea is that continental collision along the Zagros suture occurred in the Miocene [8-63-64]. Paleoceanographic constraints derived from carbon and oxygen isotopic date indicate that Neo-Tethys had a connection with the northern Indian Ocean until 14Ma [72]. This factor supports the Miocene reconstruction of Neo-Tethys by [63] and is independent of regional geological evidence. Existence of widespread shallow marine and limited deep-marine Paleocene to Miocene sediment in Zagros sub-zones is consistent with the south arm of the Tethys remaining open in to Miocene [44]. Opening of the Red Sea and the Gulf of Aden resulted in rotation of the Arabian plate with respect to Africa (Nubia ano Somalia) since 30 Ma [11-28-30]. This plate movement was responsible for oblique convergence between the Arabian plate and central Iran and final closure of Neo-Tethys.

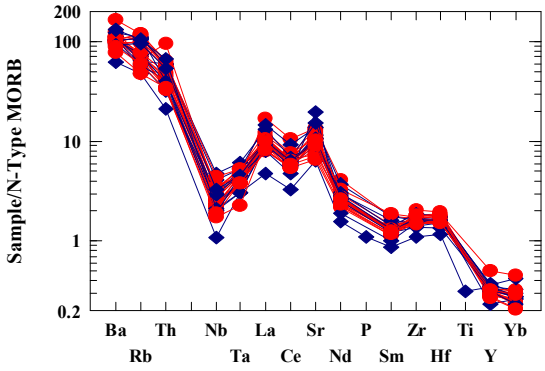

Figure 14. MORB-normalized incompatible trace element diagram for all samples [68] ♦ Andesite, ● Dacite.

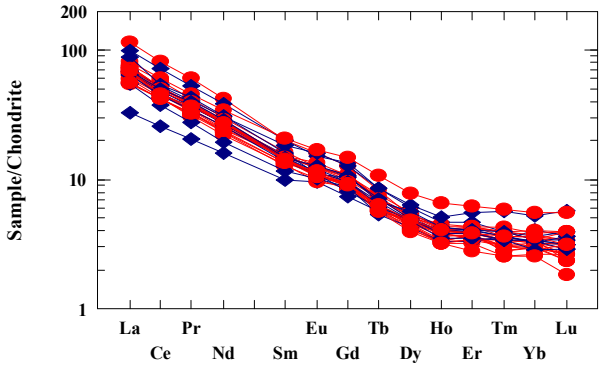

Figure 15. Chondrite-normalized REE pattern of representative dacitic samples of Central Iranian Volcanic Belt [68] ♦ Andesite, ● Dacite.

Petrological studied carried out in this area and adjacent area i.e. Mosahim, Madvar, Aj Bala, and Aj Pain indicate that post collisional magmas exhibit various geochemical enrichment signatures. The significant character of post-colllisional magmatism in this area indicates the progressive evolution of magmatic products from subalcalin to alkaline composition. A conspicuous characteristic of alkaline phase is the contemporaneous of mafic alkaline melts including melafoidites and alkali-basalts [29].

Onset of post-collisional magmatism in the late Plio-Pleistocene in this region will adakitic geochemical signatures, indicate the role of slab melting after cessation of subduction. The temporal and spatial relationship of the studied adakitic rocks may be attributed to slab roll-back and possibly break-off subducted Neo-Tethyan oceanic lithosphere beneath the Central Iranian continental microplate. Slab break-off may have led to thermal perturbation resulting in melting of detached slab and metasomatism of the mantle in Central Iran during the post-collisional event. Ascent of slab-derived magmas through thickened continental crust in this region could have been the cause of crustal contamination resulting in high Rb/Sr ratios and increase of K_2O, Th and Y contents due to assimilation and fractional crystallization (AFC) processes. Evidence for AFC processes is marked by Enrichment of K_2O over Na_2O or incompatible LILE enrichment such as Rb, Th and Ba over HFSE like Sr [22] Figure 11. The values of radiogenic Sr(0.704 to 0.705) and $\acute{\varepsilon}_{Nd}$ (+1.3 to +1.4) for this rocks respectively indicate assimilation, fractionation and crystallization processes were involved [45], this isotopic composition of adakites are similar to MORB [39].

3.2. Results

(1) In central Iran (apart of volcanice belt of Iran) numerous subvolcanic dacitic to rhyodacitic domes were intruded in to different rocks during the plio-Pleistocene.

They exhibit prophyritic texture with pheocrysts of plagioclase, hornblende and minor biotite.

(2) The geochemical characteristics of subalkaline dacitic to rhyodacitic rocks include high LILE, LREE, Sr, strongly fractionated REE patterns and low content of HREE and Y, the diagram of Y vs. Sr/Yand the diagram of $(La/Yb)_N$ vs. Yb_N showing similarities with adakites.

(3) The occurrence of adakitic among the post-collisional magmatic rocks could represent the first magmatic products after cessation of Neo-Tethys subduction in the volcanic belt of Iran.

(4) The temporal and spatial adakitic rocks and alkaline volcanic rocks in the studied area can be attributed to slab break off and melting of detached slab and metasomatised mantle.

(5) Volcanism along the dextral stike-slip faults is mainly related to extension, followed by strike-slip toctonics in the context of regional tension.

(6) The variations in K_2O, LILE and HFSE contents in comparison with modern adakites can be attributed to fractionation and crystallization processes.

Acknowledgments

This research is based on field and laboratory studies out at the University of Shahid Bahonare Kerman.I wish to acknowledge the kind support of the staff of this University.

References

1. Ahmad, T., Posht Kuhi, M. Geochemistry and petrogenesis of Urumiah-Dokhtar volcanics around Nain and Rafsanjan areas: a preliminary study. Treatise on the Geology of Iran, *Iranian Ministry of Mines and Metals*, 90p (1993).
2. Alavi, M. Tectonics of the Zagros Orogenic belt of Iran: new data and interpretations. *Tectonophysics* **220**, 211-238 (1994).
3. Alavi, M. Regional stratigraphy of the Zagros fold-thrust belt of Iran and its proforeland evolution. *American journal of Science* **304**, 1-20 (2004).
4. Amidi, S.M., Emami, M.H., Michel, R. Alkaline character of Eocene volcanism in the middle part of Iran and its geodynamic situation. *Geologische Rundschau* **73**, 917-932 (1984).
5. Atherton, M. p., petford, N. Generation of sodium-rich magmas from newly undererplated basaltic. *Nature* **362**, 144-146 (1993).
6. Berberian, F., Berberian, M. Tectono-plutonic episodes in Iran. In Gupta, H. K., Delany, F. M. (Eds.), Zagros, Hindukosh, Himalaya. Geodynamic Evolution *American Geophysical union, Washington*, DC, pp. 5-32 (1981).
7. Berberian, M., King, G. C. Towards a paleogeography and tectonics evolution of Iran. *Canadian Journal of Earth Sciences* **18**, 210-265 (1981).
8. Berberian, F., Muir, I. D., Pankhurst, R. J., Berberian, M. Late Cretaceous and early Miocene Andean type plutonic activity in northern Makran and central Iran. *Journal of Geological Society of London* **139**, 605-614 (1982).
9. Berberian, E. Oceanic evolution, rifting or drifting in the Red Sea. *Nature* **330**, 692-693 (1987).
10. Biabangard, H., Moradian, A. Geochemical Study of Dacitic Rocks from North Shahr Babak, Proceedings of the Sixth, *Symposium of Geological Society of Iran, August* **27**-29,2002, pp. 396-402 (2002).
11. Bonatti, E. Oceanic evolution, rifting or drifting in the Red Sea? *Nature*, **330**: 692-693 (1987).
12. Chung, S. L., Chu, M. F., Zhang, Y., Zie, Y., Lo, C. H.,

Lee, T. Y., Ching-Ying Lan, C.Y., Xianhua Li, X., Zhang, O., Wang, Y. Tibetan tectonic evolution inferred from spatial and temporal variations in post-collisional magmatism. *Earth Sciences Review* **68**, 173-198 (2005).
13. Cox, K. G., Bell, J. D., and Pankhurst, R. J. The interpretation of igneous rocks, *George Allen and Vnwin, London* (1979).
14. Dehghani, G. A., Makris, T. The gravity field and crustal structure of Iran. *Neues Jahrbuch fur Geologie und Palaontologie-Abhandlun-gen* **168** (2-3), 215-229 (1984).
15. Defant, J., and Drummond, S. Derivation of some modern arc magmas by melting of young subducted lithosphere, *Nature,* **374**, 662-665 (1990).
16. Defant, M.J., and Kepezhinskas, P. Evidence suggests slab melting in arc magmas. EOS Trans., 20, Am. *Geophys. Union, Washington, DC.*, **82**: 67-69 (2001).
17. Dercourt, J., Zonenenshain, L., Ricou, L.E., Kazmin, G., Lepichon, X., Knipper, A.L, Grandjacquet, C., Sbotshikov, I.M., Geyssant, J., Lepvrier, C., Pechersky, D.H., Boulin, J., Sibuet, J.C, Savostin, L.A., Sorokhtin, O., Westphal, M., Bazhenov, M.L., Lauer, J.P., and Biju-Duval, B. Geological evolution of the Tethys belt from the Atlantic to Pamirs since the Lias. *Tectonophysics* **123**: 241-315 (1986).
18. Derek, J., Thorkelson., Kartin, B. Partial melting of slab mindow margins: genesis of adakitic. *Lithos* **79**. 25-41 (2004).
19. Dimitrijevic, M. D., Dimitrijevic, M. N., Djordjevic, M., Djokovic, I. *Geological Survey of Iran*, 1:100,000 Series, Sheet 72 50, Anar (1971).
20. Dimitrijevic, M. D., and Djokovic, I. Geological map of Kerman region. (1:500000 scale), *Geological Survey of Iran* (1971).
21. Drummond, M. S., Defant, M. J. A model for trondhijemite-tonalite-dacite genesis and crustal growth via slab melting: Archaean to modern comparisons. *Journal of Geophysical Research* **95**, 21503-21521 (1990).
22. Esperanca, S., Crisci, M., de Rosa, R., Mazzuli, R. The role of the crust in the magmatic evolution of the island Lipari (Aeolian Islands. Italy). *Contributions to Mineralogy and Petrology* **112**, 450-462 (1992).
23. Farhoudi, G.H. A comparison of Zagros geology to island-arcs. *Journal of Geology* **86**, 323-334 (1978).
24. Forster, H., Fesefeldt, K., Kursten, M. magmatic and orogenic evolution of the Central Iranian volcanic belt. In: *24 th International Geology Congress, Section 2, pp*. 198-210 (1972).
25. Ghasemi, A., Talbot, C. J. A new tectonic scenario for the Sanandaj-Sirjan Zone (Iran). *Journal of Asian Earth Sciences* **26**, 683-693 (2006).
26. Gill, J.B. Orogenic andesites and plate tectonics, *Springer Verlag, Berlin*. 390p (1981).
27. Giese, P., Makris, J., Akashe, B., Rower, P., Letz, H., Mostaanpour, M. Seismic crustal studies in southern Iran between the central Iran and Zagros belt. Geodynamic Project (Geotraverse) in Iran (Final report). *Geological Survey of Iran, Report* **51**, 71-88 (1983).
28. Guiraud, R., Boswoeth, W. Phanerozoic geodynamic evolution of northeastern Africa and northwestern Arabian platform. *Tectono-physics* **282**, 39-82 (1999).
29. Hassanzadeh, J. Metallogenic and tectonomagmatic events in the SE sector of the Cenozoic active continental margin of Iran (Shahre-Babak area, Kerman Province). Unpublished Ph. D thesis, *University of California, Los Angeles*, 204pp (1993).
30. Hempton, M. R. Constraints on Arabian plate motion and extensional history of the Red Sea. *Tectonic* **6**, 687-705 (1987).
31. Hooper, R. J., Baron, I., Hatcher, J. r. R. D., Agah, S. The development of the southern Tethyan margin in Iran after the break up of Gondwana: implications of the Zagros hydrocarbon province. *Geosciences* **4**, 72-85 (1994).
32. Irvine, T. N., Baragar, W. R. A. A guide to the chemical classification of the common volcanic rocks. *Canadian Journal of Earth Sciences* **8**, 523-548 (1971).
33. Jahangiri, A. Post-collisional Miocene adakitic volcanism in NW Iran: Geochemical and geodynamic implications. *Journal of Asian Earth Sciences* **30**, 433-447 (2007).
34. Jung, D., Kursten, M., Tarkian, M. Post-Mesozoic volcanism in Iran and its relation to the subduction of the Afro-Arabian under the Eurasian plate. In: Pilger, A., Rosler, A. (Eds.), A far Between Continental and Oceanic Rifting. *Schweizerbartsche verlagbuchhand-iung Stuttgart, pp*. 175-181 (1976).
35. Kay, R. W. J. Aleutian magnesiam andesites: melts from subducted pactific oceanic crust.*Journal of Volcanology and Geothermal Research* **4**, 117-132 (1978).
36. Le Maitre, R.W., Bateman, P., Dudek, A., Keller, J., Le Bas, M. J., Sabine, P. A., Schmid, R., Sorensesen, H., Streckeisen, A., Woolley, A. R., Zanettin, B. A Classification of Igneos Rocks and Glossary of Terms. *Blackwell, Oxford,* 193pp (1989).
37. MacLean, W.H., Barrett, T.J. Lithochemical techniques using immobile elements. *Journal of Geochemical Exploration* **48**, 109-133 (1993).
38. Martin, H. The mechanism of petrogenesis of the Archean continental crust, comparison eith modern processes. *Lithos* **30**, 373-388 (1993).
39. Martin, H. The adakitic magmas: modern analogues of Archaean granitoids. *Lithos* **46** (3), 411-429 (1999).
40. Martin, H., Smithies, R. H., Rapp, R., Moyen, J. F., Champion. An overview of adakite-tonalite-trondhjemite-granodiorite (TTG), an Sanukitoid: relationships and some implications for crustal evolution, *Lithos*, **79**, 1-24 (2004).
41. Martin, H., and Hugh Rollinson. Geodynamic controls on adakite. TTG and Sanukitoid genesis:implications for modeles of crust formation, *Lithos*, **79**,1-4 (2005).
42. Maury, R. C., Sajona, F., Pubellier, M., Bellon, H., Defant, M. Fusion de la croute oceanique dans las zones de subdction/collision recentes: l' example de Mindanao (Philippines). *Bulletin de la Societe Geologique de France* **167**,579-595 (1996).
43. Middlemost, A. K. Magmas and Magmatic Racks An introduction to Igneous Petrology. *London*, (1987).
44. Mohajjel, M., Fergusson, C. L., Sahandi, M. R. Cretaceous-Tertiary convergence and continental collision, Sanandaj-Sirjan Zone ,western Iran. *Journal of Asian Earth Sciences* **21**, 397-412 (2003).
45. Moradian, A. Geochemistry, Geochronology and petrography of Feldspathoid Bearing Rocks in Urumieh-

Dokhtar Volcanic Belt, Iran Unpublished Ph. D thesis, *University of Wollongong, Australia*, 412pp (1997).
46. Peacock, S. M., Rushmer, T., Thompson, A. B. Partial melting of subducting oceanic crust. *Earth and Planetary Science Letters* **121**,224-227 (1994).
47. Pearce, J. A., Parkinson, I. J. Trace element models for mantle melting: application to volcanic are petrogenesis. In: Prichard, H. M., Albaster, T., Harris, N. B. W., Neary, C. R. (Eds.), Magmatic Processes in Plate Tectonics, vol. 76.*Geological Society of London Special Publication, pp*. **373**-403 (1993).
48. Pe-Piper,G., Piper, D. W. J. Miocene magnesiam andesites and dasites, Evia, Greece:adakites associated with subducting slab detachment and extension. *Lithos* **31**, 125-140 (1994).
49. Prouteau, G., Maury, R. C., Rangin, C., Suparka, E., Bellon, H., Pubellier, M., Cotton, J. Les adakites miocenes du NW Borneo, temoins de la fermenture de la proto-mer de Chine. C. R. *Acad. Sci. Paris* 323 serie IIa, pp.925-932 (1996).
50. Rapp, R. P., Watson, E. B., Miller, C. F. Partial melting of amphibolite/eclogite and the origin of Archaean trondhjemites and tonalities. *Precambrian Research* **51**,1-25 (1991).
51. Rapp, R. P., Shimizu, N., Norman, M. D., Applegate, G. S. Reaction between slab-derived melts and peridotite in the mantle wedge: experimental constraints at 3.8 GPa. *Chemmical Geology* **160**, 335-356 (1999).
52. Reagan, M. K., Gill, J. B. Coexisting calc-alkaline and high niobium basalts from Turrialba volcano, Costa Rica: implications for residual titanates in arc magma sources.*Journal of Geophysical Research* **94**, 4619-4633 (1989).
53. Ricou, L. E. Tethys reconstruction:plates, continental fragments and their boundaries since 260 Ma from Central America to South-eastern Asia. *Geodinamica Acta (Paris)* **7** (4), 169-218 (1994).
54. Rollinson, H. R. Using Geochemical Data: Evalution, Presentation, Interpretation.Wiley, *New York* (1993).
55. Sajona, F. G., Maury, R. C., Bellon, H., Cotton, J., Defant, M. J., Pubellier, M., Rangin, C. Initiation of subduction and the generation of slab melts in western and eastern Mindanao, Philippines. *Geology* **21**, 1007-1010 (1993).
56. Sajona, F. G., Bellon, H., Maury, R.C., Pubellier, M., Cotton, J., Rangin, C. Magmatic response to abrupt changes in tectonic setting: Pliocene-Quaternary calc-alkaline lavas and Nb-enriched basalts of Leyte and Mindanao Philippines. *Tectonophysics* **237**,47-72 (1994).
57. Sajona, F.G., Maury, R. C., Publlier, M., Letirrier, J., Bellon, H., Cotton, J. Magmatic source enrichment by slab-derived melts in a young post-collision setting, Central Mindanao (Philippines). *Lithos* **54**, 173-206 (2000).
58. Seghedi, I., Downes, H., Vaselli, O., Szakacs, A., Balogh, K., Pecskay, Z. Post-collisional Tertiary-Quternary mafic alkalic magmatism in the Carpathian-Pannonian region: a review. *Lithos* **72**, 117-146 (2004).
59. Seking, T.,Wyllie, P. J. Experimental simulation of mantle hybridization in subduction zones. *Journal of Geology* **91**, 511-528 (1982).
60. Sen, C., Dunn, T. Dehydration melting of a basaltic composition amphibolite at 1.5 and 2.0 GPa: implications for the origin of adakites. *Contributions to Mineralogy and Petrology* **117**,394-409 (1994).
61. Sen, C., Dunn, T. Experimental modal metasomatism of a spinel lherzolite and production of amphibole-bearing peridotite. *Contributions to Mineralogy and Petrology* **119**, 422-432 (1995).
62. Sengor, A. M. C. The Cimmeride Orogenic System and the Tectonics of Eurasia. *Geological Society of America Special Paper*, 195pp (1984).
63. Sengor, A. M. C., Natalin, B. A. Paleotectonic of Asia:fragments of a synthesis. In Yin , A., Harrison, T. M., (Eds.), The Tectonic Evolution of Asia Combridge University Press, *Cambridge*, 486-640 (1996).
64. Sengor, A. M. C., Altmer, D., Cin, A., Ustaomer, T., Hsu, K. J. Origin and assemble of the Tethyside orogenic collage at the expense of Gondwanaland. In: Audley-Charls, M. G., Hallam, A. (Eds.), Gondwana and Tethys. *Geological Society of London, Special Publication,* **37**,. 19-181 (1988).
65. Shahabpour, J. Island-arc affinity of the Central Iranian Volcanic Belt Journal of Asian Earth Sciences, 30, 652-665 (2007).
66. Stocklin, J. Iran central, septentrional et oriental. Lexique stratigraphique international, III, Fasicule 9b, Iran, Centre Nationnal de la Recheche Scientifique, *Paris*, 1-283 (1972).
67. Stocklin, J. Possible ancient continental margins in Iran. In: Burk, C. A., Drake, C. L., (Eds.), The Geology of Continental Margins. *Springer, Berlin*, 873-887 (1974).
68. Sun, S.S., and McDonough, W.F. Chemical and isotopic systematics of oceanic basalts: implications for mantle composition and processes. In: Saunders, A.D., and Norry, M.J., (Eds.), magmatism in ocean basins. Geol. Soc. *Londen. Spec. Pub*., **42:** 313-345 (1989).
69. Tatsumi, Y., Koyaguchi, T. An absarokite from a phlogopite-lherzolite source. *Contrib. Mineral. Petrol.*, **102**: 34-40 (1989).
70. Wilson, M. Igneous Petrogenesis: Glabal Tectonic Approach. Harper Collins *Academic*, 466p (1989).
71. Winchester, J. A., Floyd, P. A. Geochemical discrimination of immobile elements. *Chemical Geology* **20**, 325-343 (1977).
72. Woodruff, F., Savin, S. M. Miocene deep water oceanography. *Paleoceanography* **4**, 87-140 (1989).
73. Yogodzinski, G. M., Kay, R.W., Volynets, O. N., Koloskov, A. V., Kay, S. M. Magnesiam andesite in the western Aleutian Komandorsky region: implications for slab melting and processes in the mantle wedge. *Geological Society of America Bulletin* **107**(5), 505 (1995).